

## Cerium oxide nanoparticles provide radioprotective effects upon X-ray irradiation by modulation of gene expression

N. R. Popova<sup>1</sup>, T. O. Shekunova<sup>2</sup>, A. L. Popov<sup>1</sup>, I. I. Selezneva<sup>1</sup>, V. K. Ivanov<sup>2</sup>

<sup>1</sup>Institute of Theoretical and Experimental Biophysics, Russian Academy of Sciences, Pushchino, Moscow region, 142290, Russia

<sup>2</sup>Kurnakov Institute of General and Inorganic Chemistry, Russian Academy of Sciences, Moscow, 119991, Russia

nellipopovaran@gmail.com, taisia.shekunova@yandex.ru, antonpopovleonid@gmail.com, selezneva\_i@mail.ru, van@igic.ras.ru

PACS 68.65.k, 81.20.n, 82.70.Dd, 87.80.-y

DOI 10.17586/2220-8054-2019-10-5-564-572

Nanocrystalline cerium dioxide is known as a unique redox active nanomaterial. Cerium dioxide is considered as the basis for future biomedical preparations, including radioprotectors. In the framework of this study, we synthesized citrate-stabilized CeO<sub>2</sub> nanoparticles and carried out a comprehensive *in vitro* assessment of their radioprotective properties on a NCTC L929 murine fibroblast culture. It was shown that CeO<sub>2</sub> nanoparticles ensure the survival of murine fibroblasts, even after high-dose X-ray irradiation, reducing the number of dead cells in the culture and modulating the mRNA level of the key antioxidant enzymes – superoxide dismutase 1 (SOD1) and superoxide dismutase 2 (SOD2). The results obtained confirm the potential for studying the properties of CeO<sub>2</sub> nanoparticles as basic materials for designing new efficient and safe preparations for protection against ionizing radiation.

**Keywords:** cerium oxide nanoparticles, radioprotection, cytotoxicity, X-ray, ionizing radiation, fibroblasts.

Received: 22 June 2019

Revised: 4 October 2019

### 1. Introduction

Nanocrystalline cerium dioxide is a synthetic nanomaterial that is widely used in modern high-tech industries [1]. In recent years, cerium dioxide nanoparticles have been considered as one of the most promising nanobiomaterials [2]. It was shown that, due to their unique antioxidant activity, CeO<sub>2</sub> nanoparticles are able to inactivate a wide range of free radicals and reactive oxygen species (ROS) in various models of oxidative stress, including exposure to ionizing radiation [3]. It was established that unique properties of nanodispersed cerium dioxide allow this material to exhibit enzyme-like activity, for example, as a synthetic analogue of superoxide dismutase, peroxidase, haloperoxidase, phosphatase, esterase, etc. [4]. The low toxicity and high biocompatibility of nanodisperse CeO<sub>2</sub> ensure the comparative safety of its application *in vivo*, which allows one to consider this material as a promising component of drugs and medicinal preparations. We have previously found [5] that CeO<sub>2</sub> nanoparticles are able to prevent the development of oxidative stress induced by ionizing radiation not only by direct inactivation of free radicals, but also indirectly, by modulating the expression of a number of genes involved in key intracellular enzyme cascades. The unique physico-chemical characteristics of cerium dioxide nanoparticles and their biological activity make it possible to consider this nanomaterial as a promising radioprotector with a complex mechanism of protective action.

Caputo et al. have demonstrated on a HaCat keratinocyte culture that CeO<sub>2</sub> nanoparticles reduce the number of DNA breaks caused by exposure to X-ray radiation, weakening mutagenesis [6]. Wason et al. showed that activation of c-Jun terminal kinase (JNK), a key driver of radiation-induced apoptosis, was significantly enhanced by the combined action of CeO<sub>2</sub> nanoparticles and ionizing radiation in pancreatic cancer cells *in vitro*, as well as in pancreatic tumors of naked mice *in vivo* as compared to using CeO<sub>2</sub> nanoparticles or radiation therapy alone. These data demonstrate the important role of CeO<sub>2</sub> nanoparticles in the selective destruction of cancer cells and show new prospects for the use of CeO<sub>2</sub> as a radiosensitizer [7].

Xu et al. [8] showed that the intraperitoneal administration of CeO<sub>2</sub> nanoparticles to CBA/J mice exposed to radiation at a dose of 15 Gy resulted in a significant increase in their survival. In the corresponding experiments, CeO<sub>2</sub> nanoparticles were administered to mice intraperitoneally twice a week for 4 weeks. At 160 days after irradiation, 90 % of mice which received 10 μM CeO<sub>2</sub> nanoparticles injection survived, compared with 10 % survival rate for mice that did not receive the nanoparticles and 30 % survival rate for mice which received a lower dose of CeO<sub>2</sub> nanoparticles (100 nM). Zal et al. showed that CeO<sub>2</sub> nanoparticles reduced to 73 % the number of cytogenetic incidences induced

in lymphocytes by irradiation at a dose of 1.5 Gy, in comparison with the control group. The introduction of CeO<sub>2</sub> nanoparticles significantly reduced the number of apoptotic and necrotic cells in the culture of human lymphocytes [9].

Colon et al. have demonstrated the radioprotective efficacy of cerium dioxide nanoparticles (10 nM) on a culture of normal human lung fibroblasts. Cells were irradiated at a dose of 20 Gy, and after 48 hours, their viability was assessed, which correlated with the concentration of CeO<sub>2</sub> nanoparticles. At the same time, CeO<sub>2</sub> nanoparticles did not protect cancer cells of the A549 line. It is worth noting that nanocrystalline cerium dioxide was found to be superior to Amifostin – a clinically used radioprotector [10], in a series of model *in vivo* experiments performed for nude athymic mice. The radioprotective properties of nanodisperse cerium dioxide in the culture of gastrointestinal epithelium were studied [11]. The pretreatment of the culture with cerium dioxide nanoparticles provided a dose-dependent protection against radiation damage by reducing the production of ROS and increasing the expression of SOD2. It was shown [12] that the use of nanosized cerium dioxide can reduce xerostomia and dermatitis after exposure to ionizing radiation. Using two types of cell culture as examples (MCF-7 cancer cells and normal CRL-8798 cells), the selective cytotoxicity of cerium dioxide nanoparticles was revealed [13]. It was additionally shown, by the example of radiation-resistant 9L gliosarcoma cells, that the radioprotective effect of cerium dioxide nanoparticles is a function of the irradiation energy [14]. The radioprotective properties of cerium dioxide were manifested when cells treated with cerium dioxide nanoparticles were exposed to high-energy X-ray radiation. On the other hand, low-intensity radiation promoted the formation of Auger electrons by interaction with the surface of cerium dioxide nanoparticles, which significantly reduce cell viability.

The synthetic method used for CeO<sub>2</sub> nanoparticles determines their physicochemical characteristics, which in turn dictate their biological activity [15, 16]. In the framework of this study, we synthesized citrate-stabilized CeO<sub>2</sub> nanoparticles and carried out a comprehensive assessment of their radioprotective properties *in vitro* for a NCTC L929 murine fibroblast culture line.

### 1.1. Materials and methods

#### 1.2. Preparation and analysis of physicochemical properties of CeO<sub>2</sub> nanoparticles

The aqueous sol of nanocrystalline cerium oxide stabilized by citrate ions was used in the present work. It was obtained by dissolving 0.24 g of citric acid in 25 ml of 0.05 M aqueous solution of cerium (III) nitrate, which was then rapidly added with stirring to 100 ml of a 3 M ammonia solution and then kept for 2 hours [17]. Transmission electron microscopy testified that the sol consisted of weakly aggregated nearly isotropic 2 – 3 nm CeO<sub>2</sub> particles. The concentration of CeO<sub>2</sub> nanoparticles in the sol was 0.01 M. The pH value of the sol was in the range of 7.2 – 7.4. Just before biological experiments, CeO<sub>2</sub> nanoparticles were precipitated by acidifying the sol with 10 % hydrochloric acid to pH = 3, followed by centrifugation at 20 °C, at 11200 g for 10 minutes. The precipitated nanoparticles were resuspended in distilled water and re-centrifuged under the same conditions. The resulting precipitate was resuspended in the culture medium DMEM/F12 + 10 % fetal bovine serum (Gibco).

#### 1.3. Cell culture

The NCTC L929 murine fibroblasts were cultured in DMEM/F12 (1:1) medium with the addition of 10 % fetal bovine serum and 100 U/ml penicillin/streptomycin under 5 % CO<sub>2</sub> at 37 °C.

#### 1.4. MTT assay

The determination of mitochondrial and cytoplasmic dehydrogenases activity in living cells was carried out using a MTT assay based on the reduction of the colorless tetrazolium salt (3-[4,5-dimethylthiazol-2-yl]-2,5-diphenyltetrazolium bromide, MTT). After 24 hours of cell incubation with different concentrations of CeO<sub>2</sub> nanoparticles, 0.5 mg/ml of MTT reagent was introduced into the wells by replacing the culture media, followed by a standard MTT assay.

#### 1.5. Live/Dead assay

Assessment of the viability of the cells cultured in the presence of CeO<sub>2</sub> nanoparticles was performed on a Carl Zeiss Axiovert 200 microscope. An L-7007 LIVE/DEAD BacLight Bacterial Viability Kit (Invitrogen) was used for the assay, which included a SYTO 9 fluorescent dye (absorption – 420 nm, emission – 580 nm) and a propidium iodide (PI) dye (absorption – 488 nm, emission – 640 nm). The dyes were added to the medium (1 μg/ml) and the plate was placed in a CO<sub>2</sub> incubator for 15 min. Microphotographs were taken after washing the cells with a phosphate-buffered saline.

### 1.6. Confocal and scanning electron microscopy

The cells were seeded on the surface of glass slides in Petri dishes (Ibidi, Germany) at a density of  $10^3$  per  $\text{cm}^2$ . After cell seeding for 24 h,  $10^{-5}$  M of  $\text{CeO}_2$  nanoparticles was added to the culture medium. After incubation (24 h) the medium in the plates was replaced with HBSS containing DNA-tropic fluorescent dye Hoechst-33342 (excitation at 345 nm, emission at 487 nm). The morphology analysis of the cells was carried out using an upright confocal microscope LSM-510 with multiphoton excitation of fluorescence and an image analysis system.

After a 24 h cultivation period, the cells on the cover slips were washed with a 0.1 M phosphate buffer (pH 7.2) and fixed with a 2.5 % solution of glutaraldehyde in the same buffer for 2 h at room temperature to prepare the samples for scanning electron microscopy (SEM) analysis. After the samples were dehydrated in ethanol solutions (50 – 100 %) at 4 °C, ethanol was replaced with hexamethyldisilazane. The resulting preparations were studied on a Carl Zeiss NVision 40 workstation at an accelerating voltage of 0.5 kV.

### 1.7. X-ray irradiation

X-ray irradiation was conducted using an X-ray therapeutic machine RTM-15 (Mosrentgen, Russia) with a dose of 15 Gy for cell culture at a dose rate of  $1 \text{ Gy min}^{-1}$ , 200 kV voltage, 37.5 cm focal length and 20 mA current.

### 1.8. Real-time PCR

Total RNA from the sample cells was isolated using an RNA extraction kit (SINTOL, Russia). Reverse transcription reaction was carried out using a kit for RT (SINTOL, Russia). Real-time PCR amplification was performed using a thermocycler ANK-32 (SINTOL, Russia). Primers used for estimation of transcription level for the analyzed gene and glyceraldehyde-3-phosphate dehydrogenase (GAPDH) (reference gene) were supplied by SINTOL. A kit (SINTOL, Russia) containing SYBR Green I intercalating dye was used for real-time PCR. Then the threshold cycle values obtained in the result of PCR were determined (Table 1).

TABLE 1. The primers (sequence) of analyzed genes

Name of gene	Gene primers
IL-6	F: cttccatccagttgccttcttg R: ttgggagtggtatcctctgtga
CuZnSOD	F: gtaccagtgcaggacctatctt R: gtctccaacatgcctctcttcat
GAPDH	F: atgtgtccgtcgtggatctga R: cctgcttcaccaccttcttga
MnSOD	F: ccacacattaacgcgcagat R: ggtggcgttgagattgttca
Gpx-1	F: ccaccgtgtatgccttct R: gagacgcgacattctcaatga
GSR	F: aaagaagaccccatcgggctcgg R: agagaggcaatcgacatccggaa

### 1.9. Statistical analysis

The experiments were carried out in 3 – 4 replicates and analytical determinations for each sample were performed in duplicate. The results were compared with the control experiment. Methods of variation statistics were applied to estimate the reliability of the results. To assess the statistical significance, the Mann-Whitney U test was used ( $p \leq 0.05$ ). The obtained data were processed using Microsoft Excel 2007 software.

## 2. Results and discussion

Cerium oxide nanoparticles were synthesized by a facile precipitation method using citric acid as a stabilizer. TEM images (Fig. 1(a)) of  $\text{CeO}_2$  nanoparticles confirmed their ultra-small dimensions (2 – 3 nm). They have a quasi-spherical shape and are sufficiently monodisperse. Maximum optical absorbance of citrate-stabilized nanoparticles is at 320 nm (Fig. 1(b)). Dynamic light scattering allowed to determine the mean hydrodynamic radius of cerium

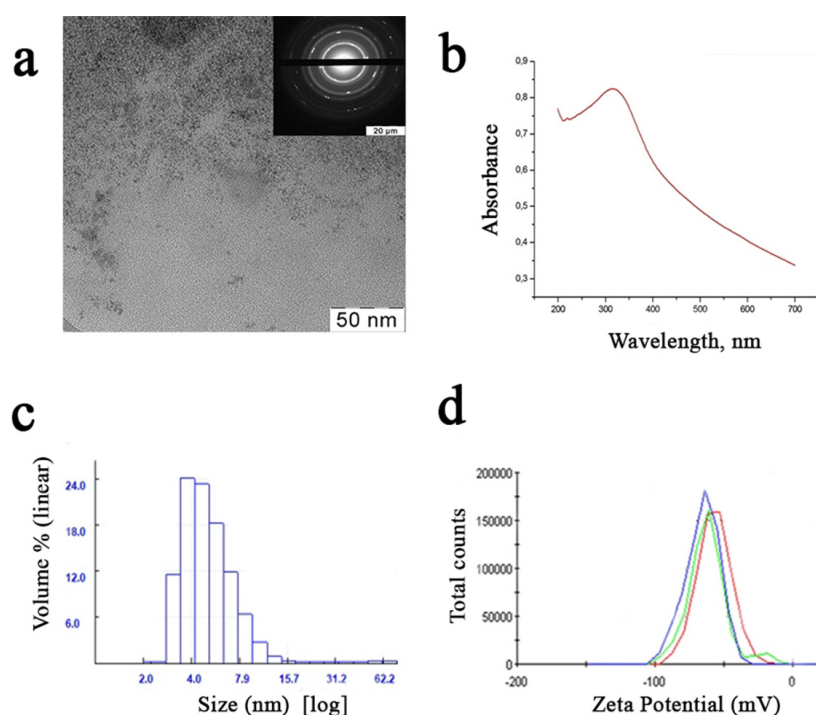


FIG. 1. image of citrate-stabilized cerium oxide nanoparticles (a), UV-vis absorption spectrum (b), hydrodynamic radii distribution of citrate-stabilized cerium oxide nanoparticles (c), potential of citrate-stabilized cerium oxide nanoparticles (d)

oxide nanoparticles diluted in DMEM/F12 + 10 % FBS culture medium, which amounted about 5 – 7 nm (Fig. 1(c)). Negative zeta potential ( $\sim -65$  mV) of  $\text{CeO}_2$  nanoparticles is provided by the citrate ions on their surface (Fig. 1(d)).

It is known that the UV-vis spectra of cerium dioxide sols can contain two absorption bands due to the presence of cerium in different valence states (+3 and +4) [18]. In the nonstoichiometric (reduced) state,  $\text{CeO}_2$  nanoparticles exhibit luminescence of Ce(III) ions at 390 nm [19]. To that end, with a decrease in  $\text{CeO}_2$  particle size, a bathochromic shift of the luminescence maximum and an increase in its intensity are observed [20]. Given these spectral characteristics of  $\text{CeO}_2$  nanoparticles, we investigated their intracellular localization by confocal microscopy. The intracellular localization of nanoparticles was confirmed (Fig. 2).  $\text{CeO}_2$  nanoparticles are distributed over the entire cytoplasm of the cell, which is shown by a characteristic green glow (Fig. 2(b)), while in the control group (without  $\text{CeO}_2$  nanoparticles) the green glow is not observed (Fig. 2(a)).

An *in vitro* study of the radioprotective effect of cerium dioxide nanoparticles was carried out using NCTC L929 murine fibroblast culture. To optimize the radiation dose, we performed preliminary studies that showed that X-rays at doses of 5 and 10 Gy do not cause damage, which are reliably detected at the cellular level after 24, 48 or 72 hours. However, a dose of 15 Gy reveals significant violations of cell structures and metabolism (40 % decrease in dehydrogenase activity according to the MTT test, morphological changes and the presence of dead cells) in a fibroblast culture within 72 hours after irradiation. It was found that preliminary incubation of NCTC L929 cell lines with  $\text{CeO}_2$  nanoparticles increases their viability (up to control values) (Fig. 3). It should be noted that all the tested concentrations of  $\text{CeO}_2$  nanoparticles ( $10^{-5}$  –  $10^{-9}$  M) increased the cell viability after irradiation in a dose-dependent manner.

A comparative analysis of cell viability using the LIVE/DEAD fluorescence test (Fig. 4) showed that preliminary treatment of cells with  $\text{CeO}_2$  nanoparticles at the concentration of  $10^{-5}$  M significantly reduces the number of dead (stained with propidium iodide) cells protecting the cell culture from the negative effects of ionizing radiation. The data obtained indicate that  $\text{CeO}_2$  nanoparticles prevent the development of oxidative stress after exposure to X-ray radiation.

The radiolysis of water that occurs in the cytoplasm of cells under the action of ionizing radiation leads to the generation of a large number of free radicals and reactive oxygen species, which damage the cellular structures, ultimately leading to its death [21]. We have previously shown that the main contribution to the radioprotective effect of  $\text{CeO}_2$  nanoparticles is precisely the decrease of intracellular ROS concentration due to chemical inactivation of water radiolysis products on the surface of nanoparticles [5]. At the same time, we revealed a complex mechanism

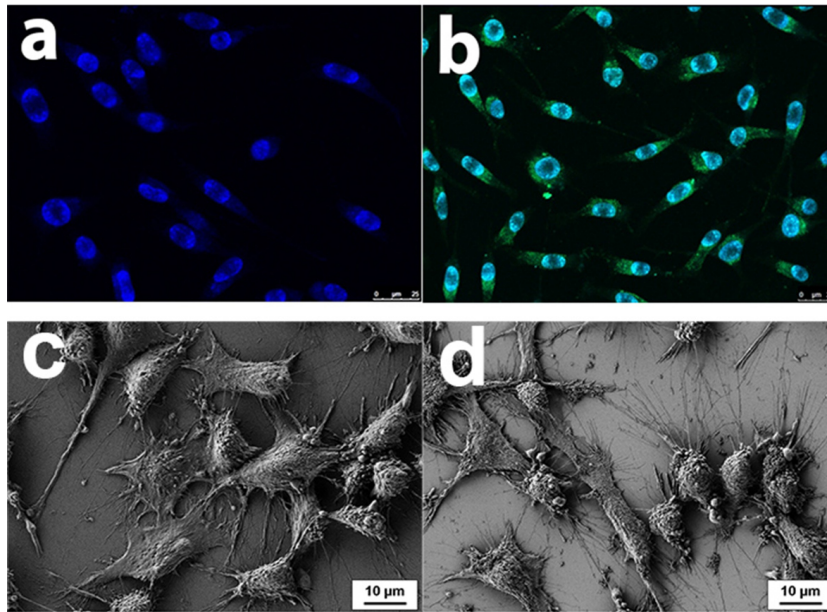


FIG. 2. Confocal images of NCTC L929 fibroblasts after 24 h exposure with cerium oxide nanoparticles (a – control, b – CeO<sub>2</sub> nanoparticles, 10<sup>-4</sup>). DAPI dye was used for nuclear staining. Morphological analysis of NCTC L929 fibroblasts after 24 h incubation with cerium oxide nanoparticles (c – control, d – CeO<sub>2</sub> nanoparticles, 10<sup>-4</sup>)

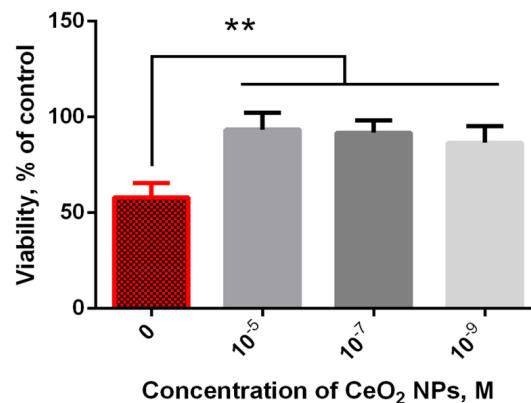


FIG. 3. Dehydrogenase activity of NCTC L929 fibroblasts after treatment with CeO<sub>2</sub> nanoparticles 72 h after exposure to X-rays at a dose of 15 Gy, as assessed by MTT-test. Control – 15 Gy without CeO<sub>2</sub> nanoparticles. \* – Significant differences estimated by the U Mann–Whitney test,  $p < 0.005$

for the radioprotective action of nanocrystalline cerium dioxide, which, in addition to chemical protection, involved physical and biological protection. The physical protection is realized through the absorption of ionizing radiation by CeO<sub>2</sub> nanoparticles and biological protection – through the activation of genes expression responsible for the development of oxidative stress in the cell.

The expression of four key antioxidant enzymes (SOD1, SOD2, glutathione peroxidase-1 and glutathione reductase) was further studied by real-time polymerase chain reaction (PCR) upon exposure of the cells to X-rays in the presence of CeO<sub>2</sub> nanoparticles (Figs. 5, 6). The glutathione reductase/glutathione peroxidase (GR/GP) system is an essential component of the body's antioxidant defence, which maintains the intensity of free radical oxidation at a stationary level [22]. Due to the GR/GP system functioning in mammalian cells, the inactivation of hydroperoxides and peroxides is achieved, which are the main source of the hydroxyl radical formed in the Fenton reaction in the presence of Fe<sup>2+</sup> ions [23]. Glutathione reductase (GR) is a common flavin enzyme that catalyzes the reversible NADPH-dependent reduction of oxidized glutathione (GSSG) [24]. The biological role of GR is to maintain a high intracellular concentration of reduced glutathione (GSH) without increasing its production.

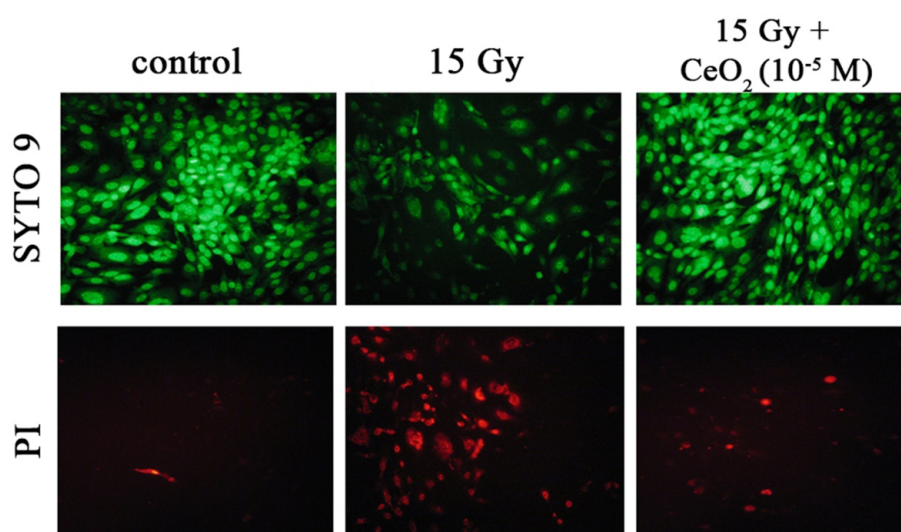


FIG. 4. Viability of murine fibroblasts (NCTC L929 cell line) treated with CeO<sub>2</sub> nanoparticles 72 h after exposure to X-rays at a dose of 15 Gy, as assessed by Live/DEAD assay. Control – cells without CeO<sub>2</sub> nanoparticles

It was shown that exposure to X-rays at a dose of 10 Gy leads to an increase in the expression of glutathione peroxidase-1 by a factor of 25 in comparison to the unirradiated control (Fig. 5). Pre-treatment of L929 cells with CeO<sub>2</sub> nanoparticles reduces the expression level of this enzyme by 2.5-fold. It can be assumed that a large number of radicals formed upon exposure to X-ray radiation are directly inactivated by CeO<sub>2</sub> nanoparticles, which exhibit activity similar to natural antioxidant enzymes of the cell including glutathione peroxidase-1. At the same time, the level of glutathione reductase transcripts remains close to the control of the treated cells, which, apparently, is associated with the need to maintain a high level of reduced glutathione after exposure to X-ray radiation. The change in the expression of Mn-superoxide dismutase (MnSOD) occurs upon incubation with cerium dioxide nanoparticles even without exposure to ionizing radiation.

Literature data [25–28] confirm the dominant role of MnSOD in protecting cells from oxidative stress induced by ionizing radiation. It was also previously shown that preincubation of colon cells [29] with CeO<sub>2</sub> nanoparticles leads to overexpression of MnSOD. There is much evidence that some forms of ROS act as signaling molecules, suggesting a much more complex role for ROS in genome expression and post-translational protein modification than it was assumed previously. For example, two transcription factors (NF-κB and AP1) are involved in intracellular redox signaling, which controls the induction of pro-inflammatory cytokines, as well as the control of the expression of MnSOD and similar antioxidants. Recent studies showed that nanocrystalline cerium dioxide is able to modulate cellular oxidative signaling pathways that are closely associated with inflammation through activation of JNK kinase, mitogen-activated protein kinase, and p38 protein [7, 30].

Using the [www.genemania.org](http://www.genemania.org) resource, we built a map of signaling pathways that involves the studied genes (Fig. 6). We conducted a study of the interleukin-6 expression – the cytokine involved in pro-inflammatory reaction. The results provide evidence that almost triple increase of expression occurs after exposure to ionizing radiation. Cerium dioxide nanoparticles do not cause an increase in the expression of the proinflammatory cytokine, and provide its reduction to the control level when exposed to ionizing radiation (Fig. 5).

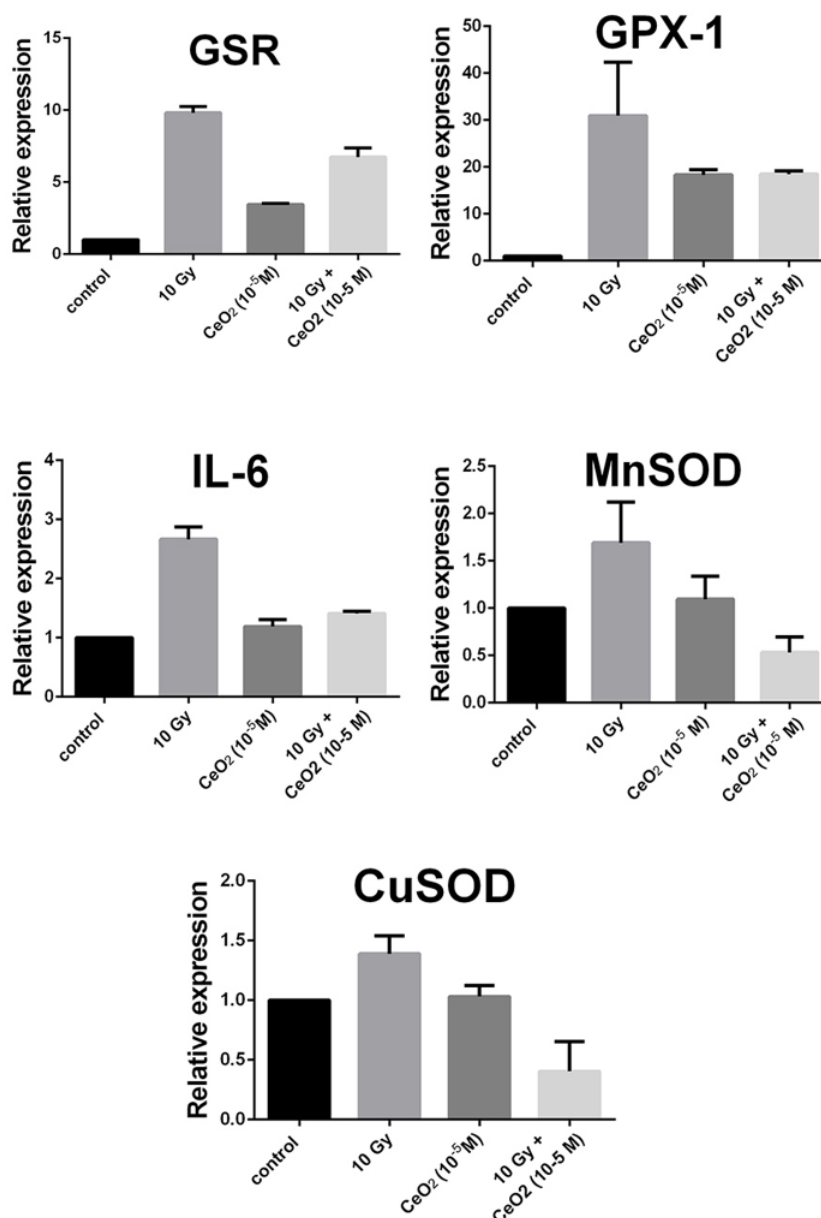


FIG. 5. Gene expression of SOD1, SOD2, GPX-1, GSR and IL-6 in murine fibroblast cell line NCTC L929 24 h after incubation with CeO<sub>2</sub> nanoparticles ( $10^{-5}$ ) and X-ray irradiation at a dose of 10 Gy

### 3. Conclusions

The data obtained indicate that cerium dioxide nanoparticles are able to modulate the expression level of key cellular antioxidant enzymes, providing a radioprotective effect upon exposure to high doses of X-rays.

### Acknowledgements

This research has been supported by the Russian Science Foundation (project 19-13-00416). Irradiation experiments were performed using the equipment of the Center of Shared Facilities of ICB RAS "Sources of ionizing radiations".

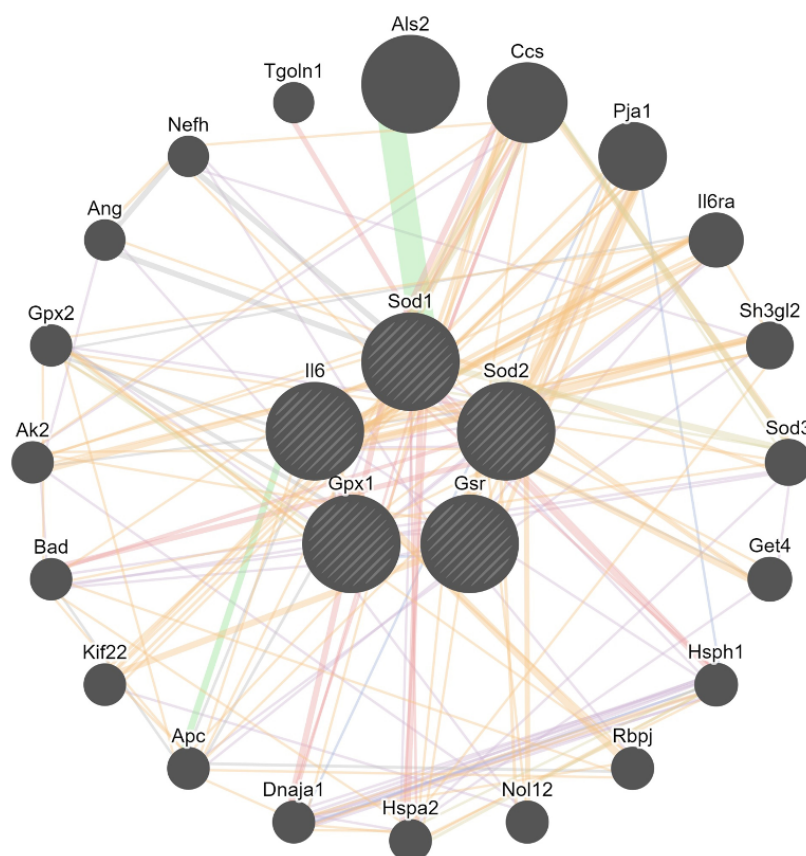


FIG. 6. Gene map of signaling pathways involved in SOD1, SOD2, GPX-1, GSR and IL-6 action

## References

- [1] Younis A., Chu D., Li S. Cerium Oxide Nanostructures and their Applications. *Intech. Open*, 2016, **3**, P. 53–68.
- [2] Shcherbakov A.B., Zholobak N., Ivanov V.K. Biological, biomedical and pharmaceutical applications of cerium oxide. In: *Metal Oxides Series: Cerium Oxide (CeO<sub>2</sub>): Synthesis, Properties and Applications*. Publisher: Elsevier, Amsterdam, 2019, P. 279–358.
- [3] Zholobak N.M., Ivanov V.K., et al. UV-shielding property, photocatalytic activity and photocytotoxicity of ceria colloid solutions. *J. Photochem. Photobiolog. B: Biology*, 2011, **102**, P. 32–38.
- [4] Popov A.L., Shcherbakov A.B., et al. Cerium dioxide nanoparticles as third-generation enzymes (Nanozymes). *Nanosystems: Physics, Chemistry, Mathematics*, 2017, **8** (6), P. 760–781.
- [5] Popov A.L., Zaichkina S.I., et al. Radioprotective effects of ultra-small citrate-stabilized cerium oxide nanoparticles in vitro and in vivo. *RSC Adv.*, 2016, **6**, P. 106141–106149.
- [6] Caputo F., Giovannetti A., et al. Cerium oxide nanoparticles re-establish cell integrity checkpoints and apoptosis competence in irradiated HaCat cells via novel redox-independent activity. *Front Pharmacol.*, 2018, **9**, 1183.
- [7] Wason M.S., Lu H., et al. Cerium oxide nanoparticles sensitize pancreatic cancer to radiation therapy through oxidative activation of the JNK apoptotic pathway. *Cancers (Basel)*, 2018, **10** (9), 303.
- [8] Xu P-T., Maidment B.W., et al. Cerium oxide nanoparticles: A potential medical countermeasure to mitigate radiation-induced lung injury in CBA/J Mice. *Radiat. Res.*, 2016, **185**, P. 516–526.
- [9] Zal Z., Ghasemi A., et al. Radioprotective effect of cerium oxide nanoparticles against genotoxicity induced by ionizing radiation on human lymphocytes. *Curr. Radiopharm.*, 2018, **11** (2), P. 109–115.
- [10] Colon J., Herrera L., et al. Protection from radiation-induced pneumonitis using cerium oxide nanoparticles. *Nanomedicine*, 2009, **5** (2), P. 225–231.
- [11] Colon J., Hsieh N., et al. Cerium oxide nanoparticles protect gastrointestinal epithelium from radiation-induced damage by reduction of reactive oxygen species and upregulation of superoxide dismutase 2. *Nanomedicine*, 2010, **6** (5), P. 698–705.
- [12] Madero-Visbal R.A., Alvarado B.E., et al. Harnessing nanoparticles to improve toxicity after head and neck radiation. *Nanomedicine*, 2012, **8** (7), P. 1223–1231.
- [13] Tarnuzzer R.W., Colon J., Patil S., Seal S. Vacancy engineered ceria nanostructures for protection from radiation-induced cellular damage. *Nano Lett.*, 2005, **5** (12), P. 2573–2577.
- [14] Briggs A., Corde S., et al. Cerium oxide nanoparticles: influence of the high-Z component revealed on radioresistant 9L cell survival under X-ray irradiation. *Nanomedicine*, 2013, **9** (7), P. 1098–1105.
- [15] Ivanov V.K., Polezhaeva O.S., et al. Synthesis and thermal stability of nanocrystalline ceria sols stabilized by citric and polyacrylic acids. *Russ. J. Inorg. Chem.*, 2010, **55** (3), P. 328–332.

- [16] Zholobak N.M., Shcherbakov A.B., et al. Panthenol-stabilized cerium dioxide nanoparticles for cosmeceutic formulations against ROS-induced and UV-induced damage. *J. Photochem. Photobiol. B*, 2014, **130**, P. 102–108.
- [17] Ivanova O.S., Shekunova T.O., et al. One-stage synthesis of ceria colloid solutions for biomedical use. *Dokl. Chem.*, 2011, **437** (2), P. 103–106.
- [18] Stoianov O.O., Ivanov V.K., et al. Determination of cerium(III) and cerium(IV) in nanodisperse ceria by chemical methods. *Russ. J. Inorg. Chem.*, 2014, **59** (2), P. 15–23.
- [19] Maksimchuk P.O., Masalov A.A., Malyukin Yu.V. Spectroscopically detected formation of oxygen vacancies in nanocrystalline CeO<sub>2x</sub>. *Journal of nano- and electronic physics*, 2013, **5** (1), 01004.
- [20] Maksimchuk P., Masalov A.A. Optically detected effect of size on the oxygen vacancies concentration in cerium oxide nanocrystals. *Proceedings of the International Conference Nanomaterials: Applications and Properties*, Alushta, 2014, **3** (2), 02NAESF05.
- [21] Le Caër S. Water Radiolysis: Influence of Oxide Surfaces on H<sub>2</sub> Production under Ionizing Radiation. *Water*, 2011, **3**, P. 235–253.
- [22] Espinosa-Diez C., Miguel V., et al. Antioxidant responses and cellular adjustments to oxidative stress. *Redox Biol.*, 2015, **6**, P. 183–197.
- [23] Zhao Y., Seefeldt T., et al. Effects of glutathione reductase inhibition on cellular thiol redox state and related systems. *Arch. Biochem. Biophys.*, 2009, **485** (1), P. 56–62.
- [24] Couto N., Wood J., Barber J. The role of glutathione reductase and related enzymes on cellular redox homeostasis network. *Free Radic. Biol. Med.*, 2016, **95**, P. 27–42.
- [25] Murley J.S., Kataoka Y., et al. Delayed cytoprotection after enhancement of SOD2 (MnSOD) gene expression in SA-NH mouse sarcoma cells exposed to WR-1065, the active metabolite of amifostine. *Radiat. Res.*, 2002, **158**, P. 101–109.
- [26] Wong G.H. Protective roles of cytokines against radiation: induction of mitochondrial MnSOD. *Biochim. Biophys. Acta*, 1995, **1271**, P. 205–209.
- [27] Hirose K., Longo D.L., Oppenheim J.J., Matsushima K. Overexpression of mitochondrial manganese superoxide dismutase promotes the survival of tumor cells exposed to interleukin-1, tumor necrosis factor, selected anticancer drugs, and ionizing radiation. *FASEB J.*, 1993, **7**, P. 361–368.
- [28] Sun J., Chen Y., Li M., Ge Z. Role of antioxidant enzymes on ionizing radiation resistance. *Free Radic. Biol. Med.*, 1998, **24**, P. 586–593.
- [29] Motoori S., Majima H.J., et al. Overexpression of mitochondrial manganese superoxide dismutase protects against radiation-induced cell death in the human hepatocellular carcinoma cell. *Cancer Research*, 2001, **61**, P. 5382–5388.
- [30] Selvaraj V., Nepal N., et al. Inhibition of MAP kinase/NF-κB mediated signaling and attenuation of lipopolysaccharide induced severe sepsis by cerium oxide nanoparticles. *Biomaterials*, 2015, **59**, P. 160–171.